Chinese Chemical Letters 32 (2021) 676–680

Contents lists available at ScienceDirect

Chinese Chemical Letters

journal homepage: www.elsevier.com/locate/cclet

Communication

Highly efficient photocatalytic Suzuki coupling reaction by Pd_3P/CdS catalyst under visible-light irradiation

Huai-Qing Yang[a,b], Qian-Qian Chen[a,b], Fulai Liu[a,b], Rui Shi[a], Yong Chen[a,b,*]

[a] *Key Laboratory of Photochemical Conversion and Optoelecctronic Materials & CAS-HKU Joint Laboratory on New Materials, Technical Institute of Physics and Chemistry, Chinese Academy of Sciences, Beijing 100190, China*
[b] *University of Chinese Academy of Sciences, Beijing 100049, China*

ARTICLE INFO

Article history:
Received 26 April 2020
Received in revised form 11 June 2020
Accepted 15 June 2020
Available online 17 June 2020

Keywords:
Pd_3P
CdS
Photocatalysis
Suzuki coupling reaction

ABSTRACT

Monodispersed palladium phosphide (Pd_3P) (5.2 ± 0.5 nm) was firstly applied to photocatalytic Suzuki coupling reaction under visible light irradiation with CdS nanoflake as a photosensitizer. This heterogeneous system exhibited high yields to corresponding products and excellent stability in alcohol solvent at room temperature.

The formation of carbon-carbon (C—C) bonds *via* coupling reactions has been applied to synthesize a wide range of organics, such as natural products, pharmaceuticals, perfumes and dyes [1–6]. Recently, photocatalytic C—C coupling reactions have attracted considerable attention due to its sustainability. Especially, Pd nanoparticles (NPs) displayed high conversion and selectivity in these photocatalytic C—C coupling reactions [7–9]. However, the relatively high cost of individual Pd NPs is disadvantageous to its widespread application [10,11]. To improve the atomic utilization, Kim and coworkers studied the size effect of Pd NPs on visible-light-driven Suzuki coupling reaction and found that 5.5 nm Pd NPs supported on exfoliated 2H-WS_2 exhibited an extraordinary photocatalytic activity, where polyvinylpyrrolidone (PVP) was used to stabilize the highly active ultrafine Pd NPs [12]. Guo and coworkers reported that PdCu alloy with a Pd/Cu molar ratio of 3:1 could not only enhance the photocatalytic activity toward Sonogashira C—C coupling reaction but also reduce the use of metal Pd [13].

Metal phosphides (MPs) are composed of zero-valent metal and phosphorus; metal-rich phosphides have similar characteristics to zero-valent metals [14]. We and others recently reported that Ni_2P, CoP, Cu_3P, *etc.* could act as excellent cocatalysts in a myriad of photocatalytic reactions for hydrogen evolution [15–17], reduction of nitroarenes [18] and CO_2 reduction [19]. In view of the fact that Pd_3P NPs have similar characteristics to Pd NPs, the following question naturally arises: Can Pd_3P NPs be used as cocatalysts for photo-driven C—C coupling reactions? Our present study shows that photocatalytic Suzuki coupling reactions are indeed highly efficient with Pd_3P as a cocatalyst, CdS as a photosensitizer, 4-iodotoluene and phenylboronic acid as the coupling partners and ethanol as an electron donor, in which a yield of up to 98% can be achieved under optimized conditions at room temperature. To the best of our knowledge, it is the first time that Pd_3P is used in catalyzing Suzuki coupling reactions. The high catalytic activity and excellent stability of this present system highlights its promising application in other cross-coupling reactions.

Pd_3P was prepared by a one-step annealing reaction of $Pd(Ac)_2$ and NaH_2PO_2 with a mass ratio of 1:5 under Ar atmosphere. As revealed by X-ray diffraction (XRD) pattern in Fig. S2 (Supporting information), the sample synthesized at 400 °C has well-defined peaks of orthorhombic Pd_3P (JCPDS No. 089-3046) [20–22] without other impurities. Further, X-ray photoelectron spectroscopy (XPS) was performed to analyze the valence state and electronic properties of Pd_3P NPs. As shown in Fig. S3c (Supporting information), two discernible peaks of P 2p region located at 129.8 eV and 130.6 eV can be assigned to P $2p_{3/2}$ and $2p_{1/2}$ of Pd_3P, respectively. The peak at 134.6 eV can be attributed to P—O bond, which originates from surface oxidation of Pd_3P [23]. Compared with the P^0 peaks at 130.1 and 131.4 eV [20,21,24], P element in

* Corresponding author at: Key Laboratory of Photochemical Conversion and Optoelecctronic Materials & CAS-HKU Joint Laboratory on New Materials, Technical Institute of Physics and Chemistry, Chinese Academy of Sciences, Beijing 100190, China.
E-mail address: chenyong@mail.ipc.ac.cn (Y. Chen).

https://doi.org/10.1016/j.cclet.2020.06.022
1001-8417/

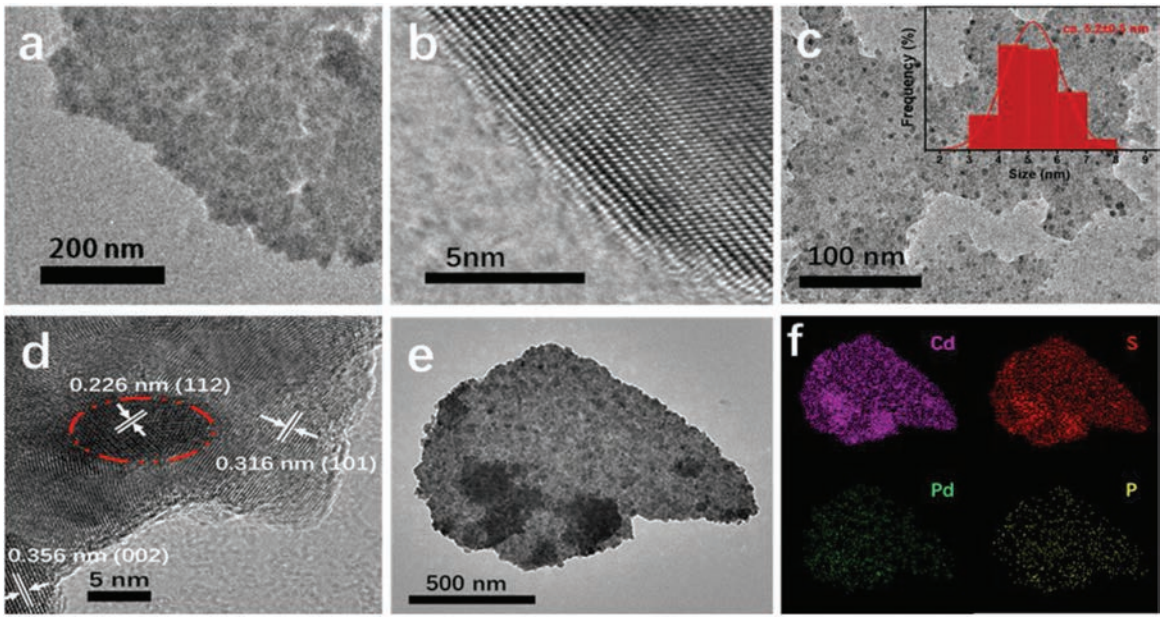

Fig. 1. (a) TEM image and (b) HRTEM image of CdS. (c) TEM image and (d) HRTEM image of Pd_3P/CdS (Inset (c): size distributions of Pd_3P NPs). (e, f) TEM image and corresponding TEM-EDS elemental mapping images of hybrid Pd_3P/CdS.

Pd_3P owns a lower binding energy, indicating its slightly negative charge in Pd_3P NPs. In addition, the peaks of Pd 3d region located at 335.9 eV and 341.2 eV belong to Pd $3d_{5/2}$ and Pd $3d_{3/2}$, respectively. Compared with binding energies (335.2 eV and 340.5 eV) of metal Pd [12,25], the higher binding energies of Pd species in Pd_3P NPs indicate that Pd element is in the form of slightly positive valence state. Finally, the effect of calcination temperature on the structure and composition of as-prepared samples was explored and corresponding XRD patterns of samples synthesized at 300 °C, 400 °C and 550 °C are shown in Fig. S2. We failed to obtain pure Pd_3P above or below 400 °C. For example, incomplete phosphidation exists in the sample synthesized at 300 °C, in which two peaks at 39.4° and 45.8° ascribed to Pd NPs are observed [26]. However, PdO and other impurities such as PdP_2 and PdO are detected in the sample synthesized at 550 °C.

CdS was fabricated *via* a hydrothermal route according to literature methods. As shown in Fig. S3a (Supporting information), XRD pattern reveals that CdS is present in hexagonal phase (JCPDS No. 77-2306) [27]. Furthermore, hybrid Pd_3P/CdS was obtained by mechanical mixing of a certain amount of Pd_3P and CdS. In the XRD pattern of hybrid Pd_3P/CdS in Fig. S3a, the weak diffraction peaks of Pd_3P at 39.9°, 40.3° and 42.6° prove that Pd_3P NPs are successfully incorporated onto CdS. Finally, to clarify the optical property of CdS, Pd_3P and Pd_3P/CdS, ultraviolet-visible diffuse reflectance spectra were performed. As shown in Fig. S3b (Supporting information), Pd_3P/CdS shows an enhanced absorption than naked CdS in the visible region.

The morphological information of CdS and hybrid Pd_3P/CdS was characterized by transmission electron microscopy (TEM). TEM image of Cds in Fig. 1a exhibits the flake-like shape. A high-resolution TEM (HRTEM) image (Fig. 1b) shows that CdS has the distinct lattice fringes, suggesting its excellent crystallinity. Obviously, as revealed by the TEM image of hybrid Pd_3P/CdS in Fig. 1c, ultrasmall Pd_3P NPs are uniformly dispersed on the surface of CdS nanosheets and the average size of Pd_3P NPs is about 5.2 ± 0.5 nm based on statistical analysis of sizes of 120 Pd_3P NPs. HRTEM image of hybrid Pd_3P/CdS is also shown in Fig. 1d. The high-resolved lattice fringes with distances of 0.316 nm and 0.356 nm can be well indexed to the (101) and (002) planes of CdS, respectively, and 0.226 nm corresponds to (112) plane of Pd_3P, which well correspond to XRD results. Meanwhile, the HRTEM result confirms the intimate contact of CdS nanosheets and Pd_3P NPs. To further prove the distribution of Pd_3P NPs on CdS nanosheet, the TEM-EDS elemental mapping images of Pd_3P/CdS are illustrated in Fig. 1f and indicate the existence and homogenous distribution of Cd, S, Pd and P elements in Pd_3P/CdS.

The performance of Pd_3P/CdS photocatalyst for photocatalytic Suzuki coupling reaction was assessed under the irradiation of white LED light (4×25 W) at room temperature. Typically, the system was constructed with 4-iodotoluene and phenylboronic acid as the coupling partners, K_2CO_3 as base, EtOH and H_2O with a volume ratio of 3:2 as solvent. As shown in Table 1, 4-iodotoluene can be converted into desirable 4-phenyltoluene with 98% yield (entry 1). Notably, the control experiments showed that the reaction could hardly occur when either components of Pd_3P, CdS, light or Pd_3P/CdS was absent (entries 2–5), which confirms that the Suzuki coupling reaction is photocatalyzed by hybrid Pd_3P/CdS under visible light. In the absence of K_2CO_3, no desirable product

Table 1
Photocatalytic Suzuki coupling reaction over Pd_3P/CdS.[a]

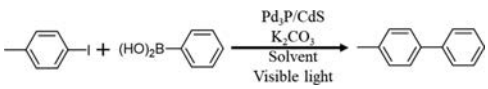

Entry	Deviation from "standard condition"	Yield (%)[b]
1	None	≥ 98
2	No Pd_3P	0
3	No CdS	Trace
4	No hv	0
5	No Pd_3P/CdS	0
6	No K_2CO_3	0
7	reflux of 80 °C instead of visible light	< 12

[a] Standard condition: 4-iodotoluene (0.1 mmol), phenylboronic acid (0.12 mmol), Pd_3P/CdS (5 mg), K_2CO_3 (0.5 mmol), EtOH/H_2O (3:2), 4×25 W LED lamp, r.t.
[b] Determined by ^1H NMR.

Table 2
Photocatalyzed Suzuki coupling reactions with various aryl halides by Pd_3P/CdS.[a]

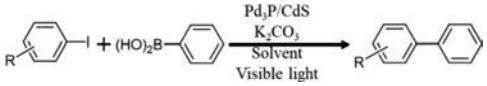

Entry	Aryl halides	Product	Time (h)	Yield (%)[b]
1		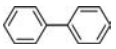	8	99
2		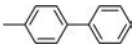	8	98
3		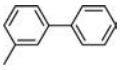	8	95
4		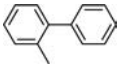	8	93
5	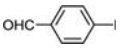	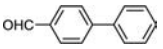	8	97
6	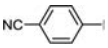	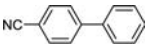	8	98
7	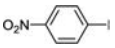	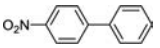	8	97
8	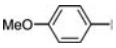	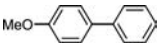	8	94
9	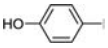	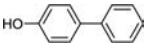	8	94
10	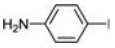	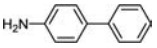	8	92
11		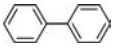	12	78
12	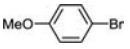	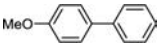	12	72
13	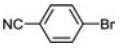	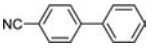	12	84
14	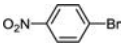	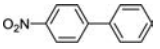	12	82

[a] Standard condition: aryl halides (0.1 mmol), phenylboronic acid (0.12 mmol), Pd_3P/CdS (5 mg), K_2CO_3 (0.5 mmol), EtOH/H_2O (3:2), 4 × 25 W LED lamp, r.t.
[b] Determined by ^1H NMR.

was detected (entry 6), because the Suzuki coupling reaction needs base to achieve deprotonation of aryl boric acid and by-product hydrogen halide [28]. Therefore, the addition of an appropriate amount of K_2CO_3 is necessary to drive this reaction. In addition, to eliminate the effect of photo-induced heat to Suzuki coupling reaction, the control experiment was carefully operated under heating condition without visible light irradiation (entry 7). Only

Table 3
Photocatalyzed Suzuki coupling reactions with several aryl-boronicacids by Pd_3P/CdS.[a]

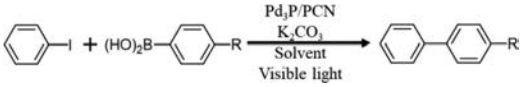

Entry	Arylboroinc acid	Product	Time (h)	Yield (%)[b]
1	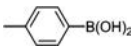	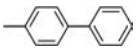	8	97
2	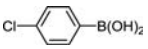	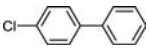	8	95
3	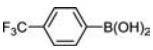	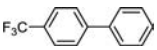	8	94

[a] Standard condition: Iodobenzene (0.12 mmol), arylboroinc acid (0.1 mmol), Pd_3P/CdS (5 mg), K_2CO_3 (0.5 mmol), EtOH/H_2O (3:2), 4 × 25 W LED lamp, r.t.
[b] Determined by ^1H NMR.

trace desirable product was detected, which further suggests that the reaction is actually photo-driven. Moreover, the cycling experiment under the "standard condition" was performed carefully. Hybrid Pd_3P/CdS after 4 cycles can maintain the activity almost equivalent to the first cycle (Fig. S4 in Supporting information), indicating its excellent stability.

With the optimal conditions in hand, we sought to evaluate the generality of photocatalytic Suzuki coupling reaction by Pd_3P/CdS. Various aryl halides and boronic acids are cross-coupled under the standard condition (Tables 2 and 3). ^1H NMR spectroscopy was used for product detection. Overall, all aryl iodides and aryl bromides showed high yields (Table 2, entries 1–14). It can be found that the position of substituents on the benzene ring has a slight effect on the product (entries 1–4), in which the yield of *para*-substituted substrate is slightly higher than that of *ortho*- and *meta*-substrates (entries 2–4). Surprisingly, whether the substituent is electron-withdrawing or electron-donating, the reaction yields are all over 90% (entries 5–10). Aryl bromides are also evaluated under the same condition, but have moderate yield even with long reaction time (entries 11–14). Aryl chlorides result in very poor yields because the strong C-Cl bond is more difficult to break [12]. Additionally, three different aryl-boronic acid compounds and 4-iodotoluene can be successfully cross-coupled, and all of them have high yields (Table 3).

Table 4
Photocatalytic Suzuki coupling reaction over Pd_3P/CdS.[a]

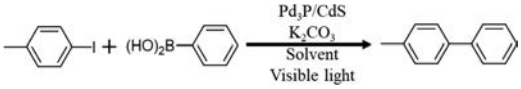

Entry	Deviation from "standard condition"	Yield (%)[b]
1	Add *p*-benzoquinone	trace
2	Add diisopropylethylamine	71
3	DMSO instead of solvent	0
4	DMF instead of solvent	0
5	MeOH instead of solvent	85
6	EtOH instead of solvent	82

[a] Standard condition: 4-iodotoluene (0.1 mmol), phenylboronic acid (0.12 mmol), Pd_3P/CdS (5 mg), K_2CO_3 (0.5 mmol), EtOH/H_2O (3:2), 4 × 25 W white LED lamp, r.t.
[b] Determined by ^1H NMR.

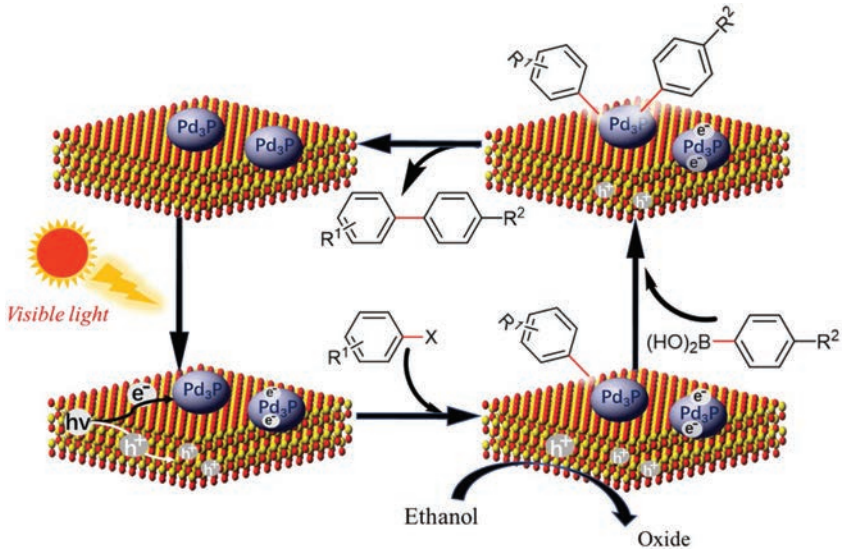

Fig. 2. Proposed mechanism responsible for photocatalytic Suzuki coupling reactions over Pd_3P/CdS.

To get an in-depth understanding of photocatalytic Suzuki coupling reaction mechanism over Pd_3P/CdS, reference experiments were performed with *p*-benzoquinone and diisopropylamine under standard condition, respectively [8,12,29]. The former is an electronic quenching agent, which competes with reactant for photoexcitation electrons from photosensitizers CdS, thus the photoexcitation electrons cannot successfully transfer to 4-iodotoluene to break C–I bonds. The latter is a good hole quenching agent, which can greatly quench the holes from photosensitizer CdS in the system and prevent the hole to transfer to phenylboronic acid. As shown in Table 4, the reaction with addition of *p*-benzoquinone can hardly proceed, whereas the yield of the corresponding product is still 71% upon addition of diisopropylamine. These results imply that photogenerated electrons play a crucial role in these photocatalyzed Suzuki coupling reactions. To further figure out the effect of solvents, the reactions in different solvents were carried out and the results were observed carefully. With ethanol and methanol as solvents, it has a high yield of more than 80%. However, there is almost no products when using DMSO and DMF, which are excellent solvents for the thermal-catalytic Suzuki coupling reaction (Table 4, entries 5 and 6) [30,31]. The experimental results indicate that the alcohol solvents (methanol, ethanol, *etc.*) play a key role in photocatalytic Suzuki coupling reaction. We speculate that alcohols may act as sacrificial agents oxidized by photogenerated holes to promote photocatalytic reaction, but holes did not transfer to phenylboronic acid [32].

Based on the above experimental results, we propose a plausible mechanism of photocatalytic Suzuki cross-coupling reaction by Pd_3P/CdS (Fig. 2). Under visible light irradiation, photogenerated electron-hole pairs can be produced and separated within CdS. Then photogenerated electrons transfer to Pd_3P to break the C–X bonds, while photogenerated holes are consumed by alcohol solvent. At the same time, oxidation addition of aryhalide can occur on the surface of Pd_3P, and then arylboronic acid undergoes transmetalation. Finally, the corresponding products are obtained by reductive elimination of intermediate species [28,33].

In summary, a highly efficient catalytic system with hybrid Pd_3P/CdS as photocatalyst was established for Suzuki coupling reaction. The reaction product was obtained in a facile way. The introduction of Pd_3P cocatalyst displayed significantly enhanced activity with bare CdS. Moreover, compared with naked metal Pd, Pd_3P achieves a reduction in the usage of noble-metal Pd. Given the sustainability, high activity and economics, Pd_3P is expected to be extended to other similar C—C coupling reactions as a highly effective catalyst.

Declaration of competing interest

The authors declare that they have no known competing financial interests or personal relationships that could have appeared to influence the work reported in this paper.

Acknowledgments

We acknowledge the financial support from the Strategic Priority Research Program of the Chinese Academy of Sciences (No. XDB17000000) and the National Natural Science Foundation of China (Nos. 21773275 and 21971250). Y. Chen acknowledges the financial support from K. C. Wong Education Foundation and the CAS-Croucher Funding Scheme for Joint Laboratories.

Appendix A. Supplementary data

Supplementary material related to this article can be found, in the online version, at doi:https://doi.org/10.1016/j.cclet.2020.06.022.

References

[1] C.W. Liu, G.C. Li, S.C. Shi, et al., ACS Catal. 8 (2018) 9131–9139.
[2] N.G. Schmidt, E. Eger, W. Kroutil, ACS Catal. 6 (2016) 4286–4311.
[3] A. Balanta, C. Godard, C. Claver, Chem. Soc. Rev. 40 (2011) 4973–4985.
[4] N. Corrigan, S. Shanmugam, J. Xu, C. Boyer, Chem. Soc. Rev. 45 (2016) 6165–6212.
[5] M. Zhang, L. Yang, H. Yang, G. An, G. Li, ChemCatChem 11 (2019) 1606–1609.
[6] H. Yang, C. Tian, D. Qiu, et al., Org. Chem. Front. 6 (2019) 2365–2370.
[7] M. Koohgard, M. Hosseini-Sarvari, Catal. Commun. 111 (2018) 10–15.
[8] Z.J. Wang, S. Ghasimi, K. Landfester, K.A.I. Zhang, Chem. Mater. 27 (2015) 1921–1924.
[9] Y.Q. Ge, P.H. Diao, X. Chen, et al., Chin. Chem. Lett. 29 (2018) 903–906.
[10] N. Kaur, G. Kaur, A. Bhalla, J.S. Dhau, G.R. Chaudhary, Green Chem. 20 (2018) 1506–1514.
[11] B. Mondal, P.S. Mukherjee, J. Am. Chem. Soc. 140 (2018) 12592–12601.
[12] F. Raza, D. Yim, J.H. Park, et al., J. Am. Chem. Soc. 139 (2017) 14767–14774.
[13] B. Wang, Y.C. Wang, J.Z. Li, et al., Catal. Sci. Technol. 8 (2018) 3357–3362.
[14] S.T. Oyama, T. Gott, H. Zhao, et al., Catal. Today 143 (2009) 94–107.

[15] S. Cao, Y. Chen, C.J. Wang, et al., Chem. Commun. (Camb.) 51 (2015) 8708–8711.
[16] S. Cao, Y. Chen, C.J. Wang, et al., Chem. Commun. (Camb.) 50 (2014) 10427–10429.
[17] S. Cao, Y. Chen, C.C. Hou, et al., J. Mater. Chem. A Mater. Energy Sustain. 3 (2015) 6096–6101.
[18] S.L. Yang, L. Peng, E. Oveisi, et al., Chem. Eur. J. 24 (2018) 4234–4238.
[19] A.T. Landers, M. Fields, D.A. Torelli, et al., ACS Energy Lett. 3 (2018) 1450–1457.
[20] Q. Qin, H. Jang, L.L. Chen, et al., ACS Appl. Mater. Interfaces 11 (2019) 16461–16473.
[21] F. Luo, Q. Zhang, X. Yu, et al., Angew. Chem. Int. Ed. 57 (2018) 14862–14867.
[22] Z.J. Wu, T. Pan, Y. Chai, et al., J. Catal. 366 (2018) 80–90.
[23] Y.Q. Ji, J.Q. Xie, Y. Yang, et al., Chin. Chem. Lett. 31 (2020) 855–858.
[24] B. Tian, B.N. Tian, B. Smith, et al., Nat. Commun. 9 (2018) 1397.
[25] S.J. Hoseini, E. Jahanshahi, R.H. Fath, Appl. Organometal Chem. 31 (2017) e3718.
[26] S. Shu, P. Wang, W. Zhang, et al., Chin. Chem. Lett. 31 (2020) 2762–2768.
[27] J.P. Ge, Y.D. Li, Adv. Funct. Mater. 14 (2004) 157–162.
[28] A.A. Thomas, A.F. Zahrt, C.P. Delaney, et al., J. Am. Chem. Soc. 140 (2018) 4401–4416.
[29] M.Q. Yang, Y. Zhang, N. Zhang, et al., Sci. Rep. 3 (2013) 3314.
[30] S.J. Sabounchei, M. Pourshahbaz, A. Hashemi, et al., J. Organomet. Chem. 761 (2014) 111–119.
[31] M. Heiden, H. Plenio, Chem. Eur. J. 10 (2004) 1789–1797.
[32] O.R. Luca, J.L. Gustafson, S.M. Maddox, et al., Org. Chem. Front. 2 (2015) 823–848.
[33] A.A. Thomas, S.E. Denmark, Science 352 (2016) 329–332.